Journal of Power Sources 196 (2011) 4364–4369

Contents lists available at ScienceDirect

Journal of Power Sources

journal homepage: www.elsevier.com/locate/jpowsour

Influence of calcination temperature and atmosphere preparation parameters on CO-PROX activity of catalysts based on CeO_2/CuO inverse configurations

Antonio López Cámara[a], Anna Kubacka[a], Zoltán Schay[b], Zs. Koppány[b], Arturo Martínez-Arias[a,*]

[a] Instituto de Catálisis y Petroleoquímica, CSIC, C/Marie Curie 2, Campus de Cantoblanco, 28049 Madrid, Spain
[b] Institute of Isotopes, Hungarian Academy of Sciences, H 1525 Budapest, Hungary

ARTICLE INFO

Article history:
Received 30 July 2010
Received in revised form
17 September 2010
Accepted 29 September 2010
Available online 7 October 2010

Keywords:
CO-PROX
CeO_2/CuO
TG-DTA
XRD
TPR
DRIFTS

ABSTRACT

Catalysts based on inverse CeO_2/CuO configurations employed for preferential oxidation of CO in a H_2-rich stream have been explored with respect to optimization of preparation parameters like calcination temperature and atmosphere. For this purpose, the catalysts precursors prepared by microemulsion have been characterized by TG-DTA, DRIFTS and XRD in order to select most adequate conditions. Selected specimens were further analysed by S_{BET} measurements as well as with respect to catalytic and redox properties by activity measurements and H_2-TPR tests. Activity differences are explained on the basis of textural, chemical and structural characteristics of the catalysts as a function of variations in the mentioned preparation parameters, with optimum properties being achieved for the specimen calcined under air at 500 °C.

1. Introduction

Production of H_2 for polymer fuel cells (PEMFC) is usually accomplished by a multi-step process that includes catalytic reforming of hydrocarbons or oxygenated hydrocarbons followed by water gas-shift (WGS) [1,2]. The gas stream obtained after these processes presents in most cases a relatively high CO concentration that disallows efficient handling of the fuel by the Pt alloy anode usually employed in the PEMFC. Preferential (or selective) oxidation of CO (CO-PROX process) has been recognized as one of the most straightforward and cost-effective methods to achieve acceptable CO concentrations (below *ca.* 100 ppm) [3–5]. Among different types of catalysts that have shown their ability for this process (based on Pt or Au), a group constituted by catalysts based on closely interacting copper oxide and ceria (or structurally related cerium-containing mixed oxides) has shown promising properties in terms of activity, selectivity and resistance to CO_2 and H_2O, while their lower cost could make them strongly competitive [3,5–7].

It is generally agreed that optimum catalytic properties for CO oxidation over copper–ceria catalysts are achieved in the presence of well-dispersed copper oxide patches over ceria nanoparticles [6–8]. This has been recently rationalised by spectroscopic analysis under reaction conditions of catalysts of this type showing that active sites for such reaction, under CO-PROX conditions, are related to interfacial copper oxide entities which become partially reduced during the course of interaction with the reactant mixture, for which process ceria apparently plays an important promoter role [9,10]. In turn, such studies have shown that H_2 oxidation, main reaction competing for the available oxygen with the CO oxidation one over this type of catalysts (their respective relative activity therefore determining the width of practical conversion window, i.e. temperature range at which values close to 100% CO conversion with the lowest possible H_2 oxidation activity becomes achieved), is apparently promoted when the reduction of the copper oxide particles becomes extended to non-interfacial sites, suggesting that the performance for such reaction can strongly depend on morphological characteristics of the copper oxide particles themselves [7,9]. Such results, suggesting a possible separation (at least to a certain extent; it must be noted that both oxidation processes cannot most likely be treated as fully independent [7,11,12]) between most active sites for the two main oxidation reactions (of CO and H_2, respectively) taking place along the CO-PROX process, obviously provide a key to modulation of the overall CO-PROX behaviour of this kind of systems [9]. On this basis, a recent work shows that enhanced catalytic properties can be achieved by using, instead of traditional direct catalyst configurations, in which copper oxide is dispersed onto ceria, inverse configurations in which large size copper oxide particles act as the support for ceria [13]. Such enhanced

* Corresponding author. Tel.: +34 915854940; fax: +34 915854760.
E-mail address: amartinez@icp.csic.es (A. Martínez-Arias).

0378-7753/$ – see front matter © 2010 Elsevier B.V. All rights reserved.
doi:10.1016/j.jpowsour.2010.09.085

behaviour appears rooted on the shift of hydrogen oxidation conversion to higher temperature produced as a consequence of the relatively large copper oxide particles present in the inverse configuration and considering the fact that the reducibility of copper oxide particles with hydrogen is expected to decrease with increasing particle size [12–14].

A step further concerns optimization of preparation parameters for such inverse configurations. In this sense, following a preparation method based on reverse microemulsions, by which inverse configurations of this type of systems have been shown to be achieved [13], the present study explores the influence of temperature and atmosphere (oxygen or inert) employed during calcination of the precursor, obtained after precipitation of the components within the reverse microemulsions and drying, on the CO-PROX performance of the catalysts. It must be noted in this sense that such parameters can significantly affect the catalytic properties of oxide systems by changing various physico-chemical parameters like, among others, the hydroxylation degree, the textural characteristics or the type of exposed faces. A recent example in this sense is provided by cobalt oxide which displays strong differences in CO oxidation activity as a function of such parameters, being possible to achieve a very active system upon their optimization [15,16].

2. Experimental

Inverse CeO_2/CuO and CeO_2/(Cu–Mn)O (with Cu:Mn atomic ratio of 9:1) catalysts (with Ce:(Cu + Mn) atomic ratios of 4:6; the samples will be denoted hereafter as Cu_6Ce_4 and $(Cu_9Mn_1)_6Ce_4$, respectively) were prepared by employing reverse microemulsions containing *n*-heptane, Triton-X-100 and *n*-hexanol as organic solvent, surfactant and cosurfactant, respectively, in amounts similar to those reported previously [10]. The required amount of $Cu(NO_3)_2$ (or $Cu(NO_3)_2 + Mn(NO_3)_2$) was dissolved in distilled water and added to the former in order to form the reverse microemulsion. Simultaneously, another microemulsion of similar characteristics was prepared containing dissolved in its aqueous phase the required amount of tetramethyl ammonium hydroxide (TMAH). After 1 h stirring of the two microemulsions, the TMAH-containing one was added to the Cu-containing one and it was left for the period of 18–24 h in order to complete the precipitation reaction. Then, the resulting microemulsion was heated gently up to 60 °C using a water bath. This microemulsion containing the precipitated copper (or copper and manganese) was then mixed with another one of similar characteristics in which Ce had previously been precipitated following mixing of cerium nitrate- and TMAH-containing microemulsions. This final microemulsion containing both precipitated Cu (or Cu + Mn) and Ce components was kept under agitation for the period of 18–24 h. The resulting solid was then separated by centrifugation and decantation, rinsed with methanol and dried overnight at 100 °C. This specimen will be hereafter referred to as the precursor. Chemical analysis by ICP-AES confirmed quantitative precipitation of all components. Calcinations under diluted oxygen (20% in N_2) or inert gas at selected temperatures was done during 2 h following ramps up to the desired temperature of 5 °C min^{-1}.

S_{BET} specific surface area of the catalysts was determined from N_2 adsorption isotherms of the specimens preoutgassed during 12 h at 140 °C which were recorded with automatic equipment Micromeritics 2100.

Thermogravimetric and differential thermal analyses (TG-DTA) of the precursor decomposition were performed on a Perkin-Elmer TGA7 and a Perkin-Elmer DTA7 devices, respectively, from 20 to 900 °C at a heating rate of 10 °C min^{-1} and under an air or He flow of *ca.* 60 ml min^{-1}.

XRD patterns of the samples were recorded on a Seifert XRD 3000P diffractometer using nickel-filtered CuKα radiation operating at 40 kV and 40 mA using a 0.02° step size and 2 s counting time per point. Analysis of the diffraction peaks was done with the computer program X'Pert HighScore Plus version 2.2.1. A reaction chamber allowing heating of the samples up to 700 °C under controlled atmosphere was used for these XRD experiments.

DRIFTS spectra were recorded using a Bruker Equinox 55 FTIR spectrometer equipped with a liquid N_2 cooled high sensitivity MCT detector and a Harrick Praying Mantis DRIFT cell. All spectra were recorded with an accumulation of 20 scans at a resolution of 4 cm^{-1}. Aliquots of *ca.* 100 mg catalyst were placed in a sample cup inside the DRIFTS cell with CaF_2 windows and a heating cartridge that allowed samples to be heated up to 550 °C.

Temperature programmed reduction (TPR) was measured in a flow system using 1%H_2/Ar premixed gases with flow rate of 30 mL min^{-1}, respectively. A cold trap filled with liquid nitrogen was placed after the reactor to remove water. The system was equipped with a thermal conductivity detector. About 40 mg catalyst was placed into a quartz U-tube and calcined in 5% O_2/He at selected temperatures (the same as calcination temperature respectively used) for 1 h using 40 ml min^{-1} flow rate and 10 °C min^{-1} ramp. The sample was cooled to room temperature, purged with Ar and after switching to the reducing gas mixture it was heated to 500 °C using 10 °C min^{-1} ramp.

The catalysts calcined in situ (under He or oxygen diluted in He at the calcination temperatures employed in each case) were tested in a glass tubular catalytic reactor for their activity under an atmospheric pressure flow (using mass flow controllers to prepare the reactant mixture) of 1% CO, 1.25% O_2 and 50% H_2 (Ar balance), at a rate of 1×10^3 cm^3 min^{-1} g^{-1} (roughly corresponding to 80,000 h^{-1} GHSV) and using a heating ramp of 5 °C min^{-1} up to 300 °C. Analysis of the feed and outlet gas streams was done by gas infrared (Bruker Equinox 55 FTIR spectrometer, coupled to a multiple reflection transmission cell—Infrared Analysis Inc. "long path gas minicell", 2.4 m path length, *ca.* 130 cm^3 internal volume-) and mass spectrometry (Pfeiffer Omnistar spectrometer connected on line). No products other than those resulting from CO or H_2 combustion (i.e. CO_2 and H_2O; only a residual contribution of possible WGS, taking place in any case at temperatures higher than *ca.* 200 °C, was estimated from the results obtained) were detected in the course of the runs.

3. Results and discussion

In order to select calcination temperatures, the precursors were analysed by TG-DTA under air or inert gas flow, as shown in Fig. 1. Calcination under air produces a small weight loss below *ca.* 185 °C and a very strong loss at that temperature, profiles being fairly similar for the two systems. Following such step, a small gradual loss is observed for both systems up to *ca.* 400 °C with residual losses being produced above this temperature. According to DTA analysis, basically three steps can be observed, fairly coinciding with weight losses observed in the TG profiles. Thus, weight loss below 185 °C appears related with an endothermic process which may well correspond to water desorption from the samples surface. A strongly exothermic process correlates with the strong weight loss detected at *ca.* 185 °C. This may well correspond to combustion of organic residues from the microemulsion which could not be eliminated during the drying step. A shoulder between *ca.* 350 and 400 °C reflects the presence of an exothermic process corresponding to weight losses produced above *ca.* 230 °C, which may correspond to formation of the corresponding oxides, as will be discussed below.

Important differences are encountered when the precursors are treated under inert gas flow. Thus, following the initial relatively small weight loss below *ca.* 180 °C, which as for samples treated under air can correspond to surface water desorption, in agree-

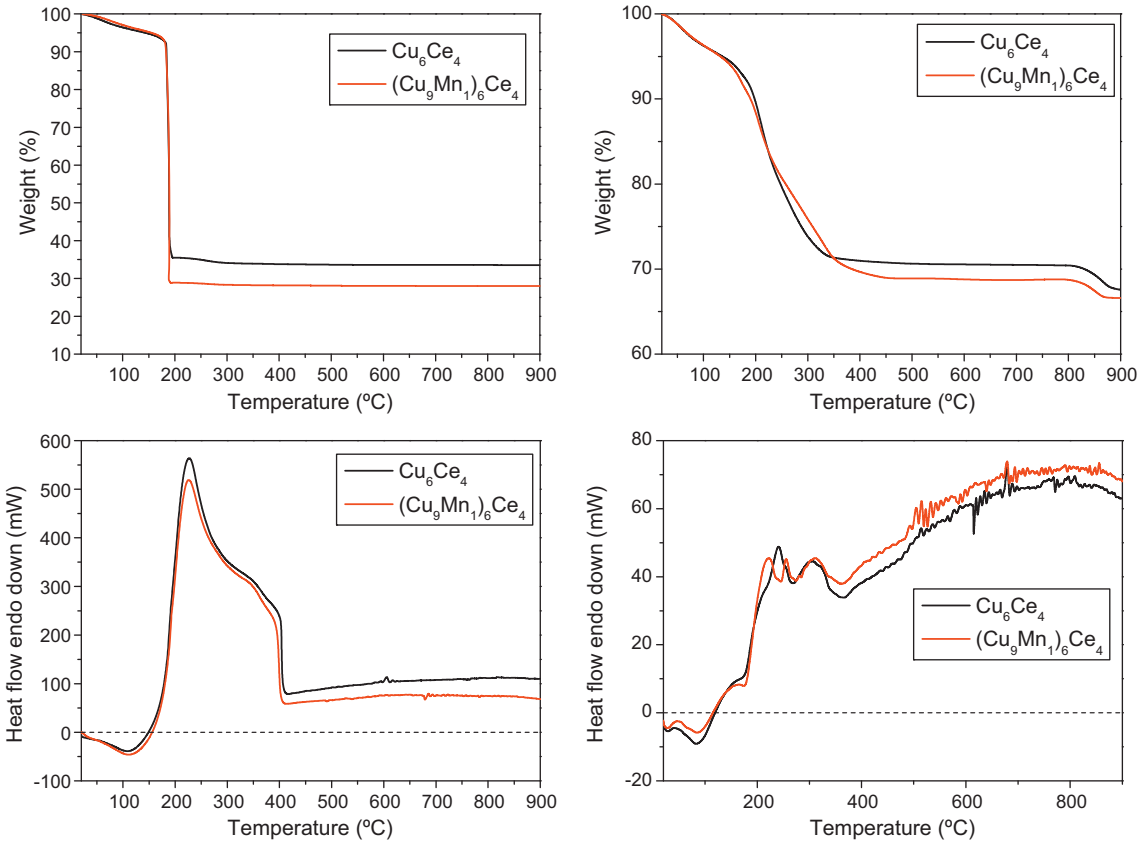

Fig. 1. TGA (top) and DTA (bottom) curves for the indicated catalysts precursors. Left: under air; right: under inert gas.

ment with its endothermic character, a large weight loss is observed between *ca.* 180 °C and 450 °C most of them apparently corresponding to exothermic steps, according to DTA results. A final small weight loss is observed above *ca.* 800 °C. Strong similarities are also found in this case between the two analysed samples, on the basis of observation of basically similar steps in the TG and DTA profiles. An important difference between the two calcination atmospheres concerns the fact that an appreciably lower overall weight loss is produced during the calcination under inert gas, suggesting that part of the microemulsion-derived organic matter may not be fully decomposed in such atmosphere.

In order to explore this hypothesis, the $(Cu_9Mn_1)_6Ce_4$ precursor has been examined by DRIFTS. As shown in Fig. 2, the initial sample displays bands related to organic residues (C–H stretching bands in the *ca.* 3000–2800 cm^{-1} zone and most intense bands related to C–O stretching in the 1700–1200 cm^{-1} region) and hydroxyls or chemisorbed water bands (*ca.* 3800–3000 cm^{-1} region). No important changes are produced under diluted oxygen flow up to 150 °C. However, an important decrease of bands related to organic matter is produced above that temperature, in agreement with TG-DTA results. An important amount of water (along with CO_2, not shown) is produced upon decomposition of such residues, which is reflected in an important increase of chemisorbed water bands at *ca.* 3400 and 1640 cm^{-1} in the spectrum recorded at 250 °C. In any case, significant decreases in organic matter, hydroxyls or chemisorbed water bands is produced up to 550 °C, as reflected also in the spectrum recorded at room temperature after cooling under the same flow. It may be noted that full disappearance of complexes derived from organic matter decomposition is not achieved up to 550 °C, which may be related to the strongly basic character of ceria which tends to retain carbonate-type species [17]. When the same sample is heated under He flow, the results show a similar trend although the amount of organic matter remaining at the end of the test up to 543 °C is apparently higher than under diluted oxygen (Fig. 3), thus evidencing the difficulties to decompose such residues under inert gas atmosphere.

XRD results regarding the evolution of crystalline phases during the course of treatment of the $(Cu_9Mn_1)_6Ce_4$ precursor under air or inert gas is displayed in Figs. 4 and 5. The structure of the precursor is basically amorphous below about 200 °C in any case. Above that temperature small crystals of CuO begin to form which increase their size up to 650 °C. Ceria crystals apparently begin to form at the same or slightly higher temperature than CuO crystals, increasing their size with increasing calcination temperature. Main differences between the two treatments are related to copper-containing phases. On the one hand, CuO crystals formed under inert atmosphere are apparently larger than those formed under air. On the other hand, an important amount of metallic copper is apparently formed under inert atmosphere above *ca.* 250 °C.

On the basis of the results so far obtained, different calcination temperatures and atmospheres were selected for further analysis (Table 1). As expected, the calcination temperature has a marked effect on S_{BET} values, as collected in Table 1. An acute decrease in this parameter is observed above 500 °C while the

Table 1
S_{BET} values observed for $(Cu_9Mn_1)_6Ce_4$ as a function of temperature and calcination atmosphere.

Calcination temperature (°C)	Calcination atmosphere	S_{BET} ($m^2\ g^{-1}$)
300	Air	190
400	Air	151
500	Air	120
600	Air	27
500	He	112

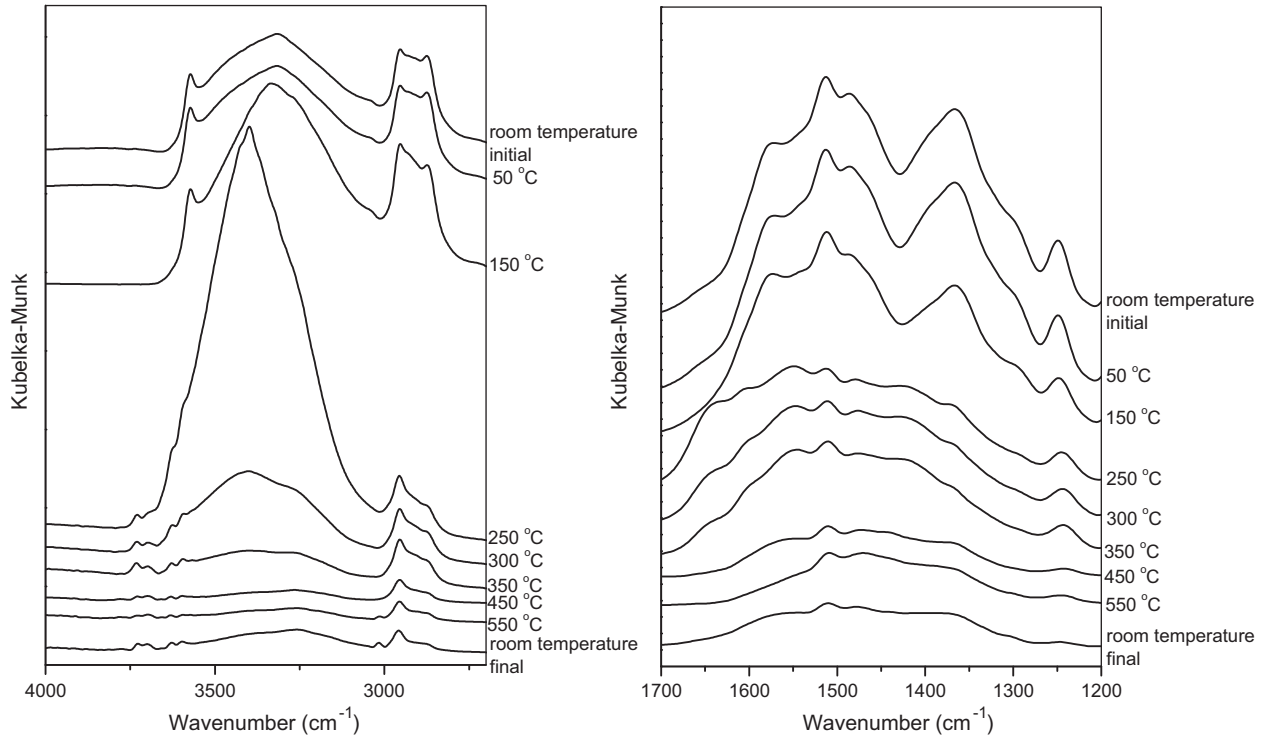

Fig. 2. DRIFTS spectra during calcination of the $(Cu_9Mn_1)_6Ce_4$ precursor under 20% O_2 in He at the indicated temperatures.

calcination atmosphere does not appear to affect it in a strong way when comparing samples calcined at 500 °C. On the other hand, analysis of X-ray diffractograms for the two samples calcined at 500 °C (not shown) for which sufficient crystallinity degree is attained within this series yields a lattice parameter for the ceria phase of 5.385 Å (fairly independent on the calcination atmosphere employed), slightly lower than expected for pure ceria. This suggests that some incorporation of Cu^{2+} cations to the ceria lattice may have taken place, taking into account the smaller size of Cu^{2+} with respect to Ce^{4+} cations [18]. In contrast, metallic Cu or CuO phases present in these samples show lattice parameters similar to those expected for the corresponding pure phases. Crystal sizes for the two samples calcined at 500 °C show values (as derived from use of the Scherrer equation) of 3.5 and 8.7 nm for the ceria and

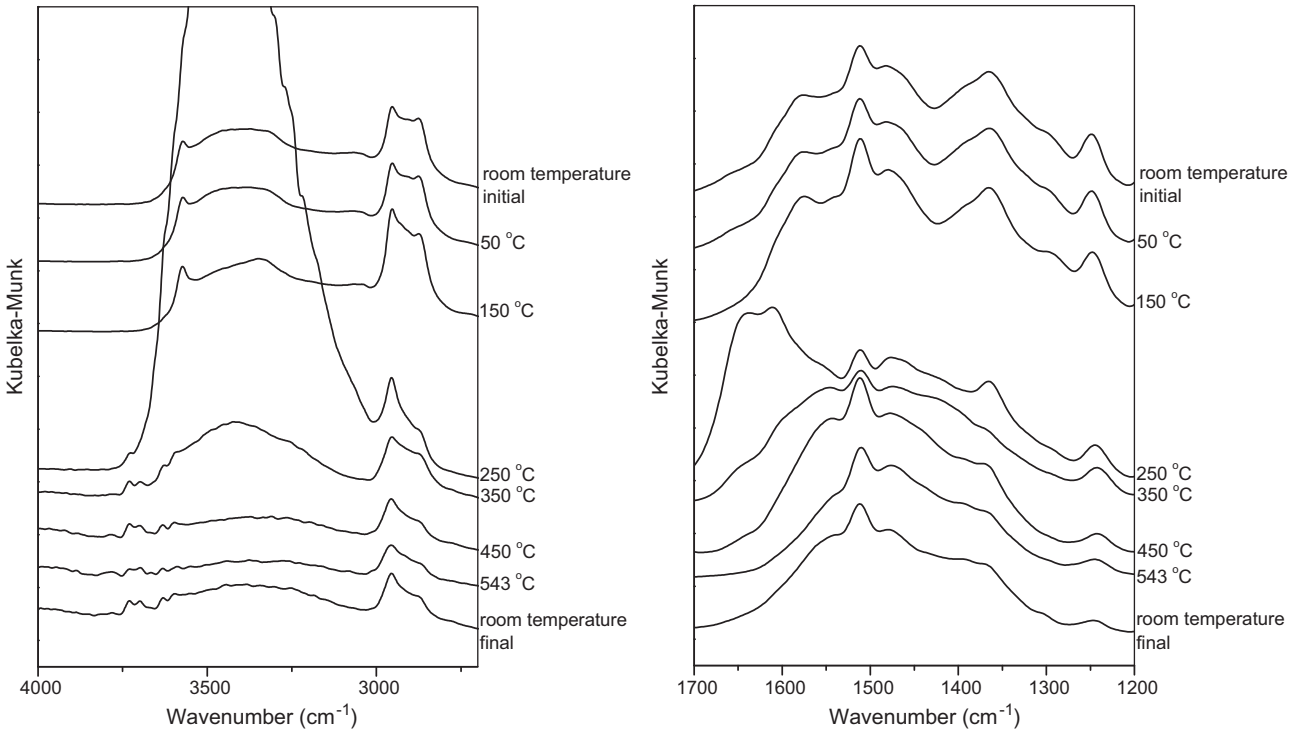

Fig. 3. DRIFTS spectra during calcination of the $(Cu_9Mn_1)_6Ce_4$ precursor under He at the indicated temperatures.

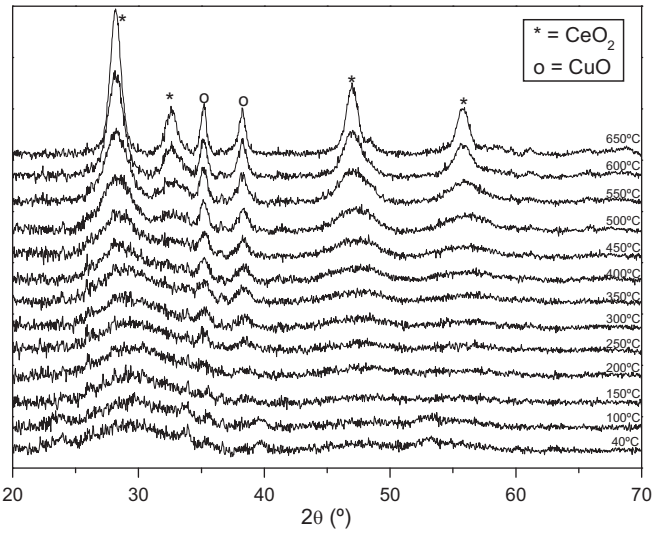

Fig. 4. X-ray diffractograms of the $(Cu_9Mn_1)_6Ce_4$ precursor recorded under air at the indicated temperatures.

CuO phases, respectively, in the sample calcined under air, and 3.1 and 14.2 nm for the ceria and metallic Cu phases, respectively, in the sample calcined under inert gas.

Catalytic activity results under CO-PROX conditions for the selected samples are displayed in Fig. 6. Noteworthy, no strong differences in terms of CO conversion are detected between samples calcined under air at 300–500 °C, in spite of the important specific surface area decrease observed (Table 1). However, the catalyst calcined under air at 600 °C displays very poor CO conversion activity, which must be mainly a consequence of the important sintering produced at that temperature (Table 1). These results contrast with those observed for other catalysts based on combinations between copper and ceria and prepared by conventional co-precipitation, in which increasing the calcination temperature up to 700 °C induced CO-PROX activity enhancement in general terms [19]. Certainly, differences in the preparation method and specific conditions employed during calcination treatments can be most relevant in explaining such different behaviours. On the other hand, the catalyst prepared under inert gas atmosphere at 500 °C displays apparently poorer CO oxidation activity than its counterpart calcined under air at the same temperature. In principle, two effects could explain such result. First, metallic copper present in the system calcined under inert gas (Fig. 5) can be less active than oxidised copper taking into account that active sites for CO oxidation under CO-PROX conditions have been related with oxidised copper species [9]; formation of metallic copper could also induce a significant sintering of the copper phase, thus decreasing the amount of copper–ceria interfacial sites responsible for such activity [9]. In second place, the presence of organic residues that could act as catalytic poisons should also be considered, taking into account TG-DTA and DRIFTS analyses exposed above (Figs. 1–3).

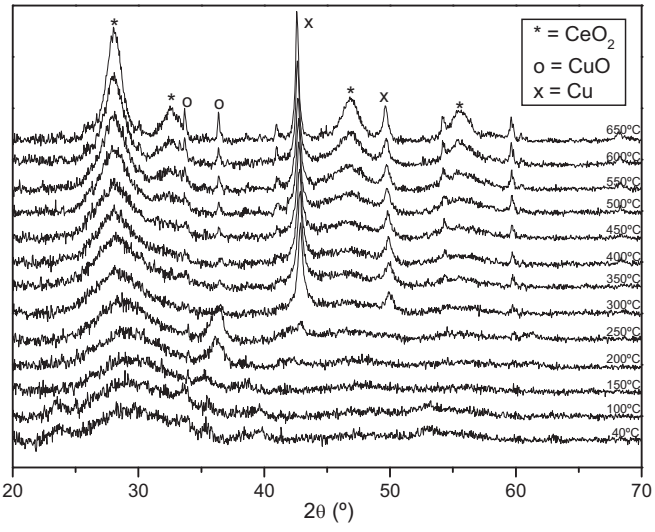

Fig. 5. X-ray diffractograms of the $(Cu_9Mn_1)_6Ce_4$ precursor recorded under He at the indicated temperatures.

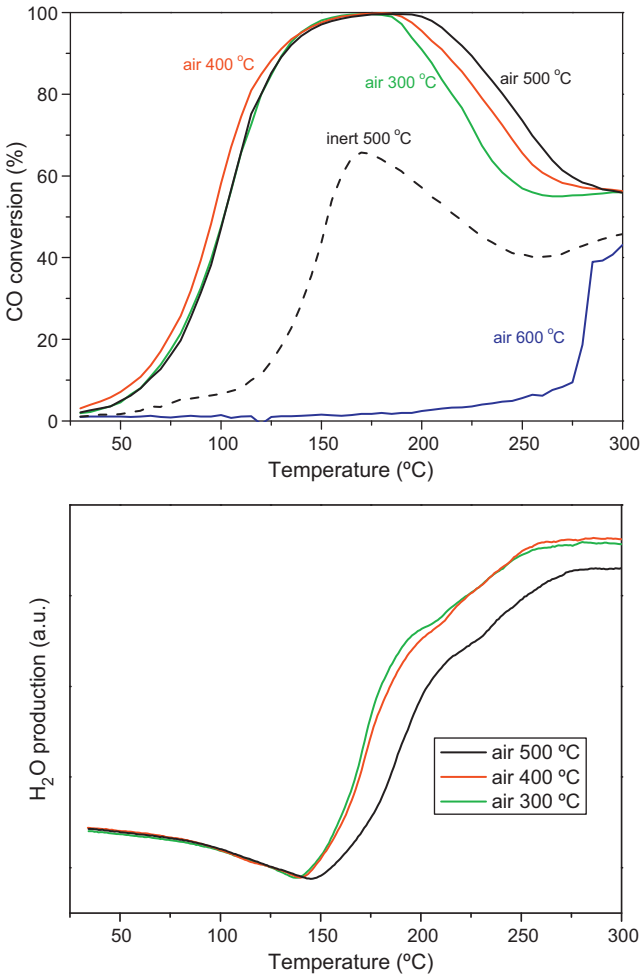

Fig. 6. Top: CO conversion activity under the $CO–H_2–O_2$ CO-PROX mixture for $(Cu_9Mn_1)_6Ce_4$ treated under indicated conditions. Bottom: H_2O production detected under the $CO–H_2–O_2$ CO-PROX mixture for $(Cu_9Mn_1)_6Ce_4$ treated under indicated conditions.

Nevertheless, selectivity differences are evident between the three samples calcined under air between 300 and 500 °C. H_2O evolution detected during the tests, which is related to respective activity for the H_2 oxidation reaction, evidences such differences. As shown in Fig. 6, H_2 oxidation activity increases with the decrease in calcination temperature in this range, thus determining the higher selectivity towards CO_2 formation of the catalyst calcined at 500 °C. This latter is therefore the one presenting optimized characteristics for the CO-PROX process. The observed behaviour can be related to differences in copper oxide reducibility under H_2, known to increase upon decreasing the particle size [12,14]; indeed, CuO particle size effects on selectivity enhancement in this sense was already pointed out earlier [5]. In order to explore this issue, these systems were analysed by H_2-TPR, as shown in Fig. 7. The three

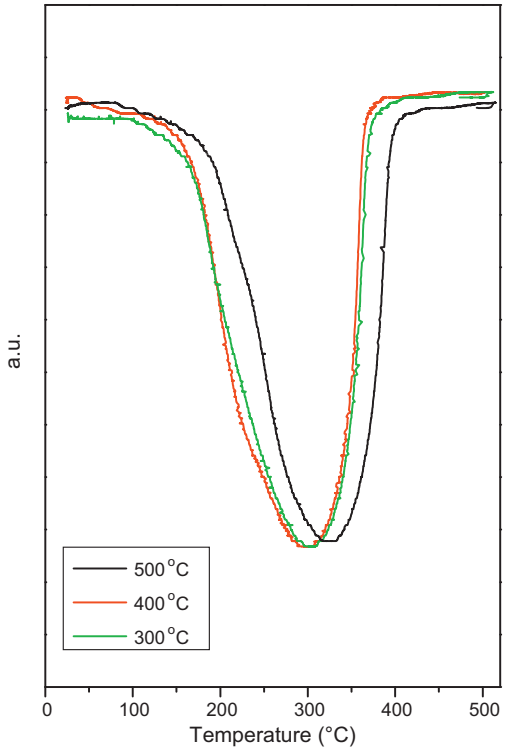

Fig. 7. H_2-TPR profiles for the $(Cu_9Mn_1)_6Ce_4$ catalyst calcined under air at the indicated temperatures.

systems display peaks at relatively high temperature (between *ca.* 300 and 330 °C), typical for relatively large CuO particles as those present in the catalysts (Fig. 4) [12,14]. However, samples calcined at 300 and 400 °C are apparently more reducible showing about 20–30 °C shift in onset of reduction as well as peak maximum, in good agreement with catalytic activity results obtained (Fig. 6).

4. Summary and conclusions

The influence of preparation parameters like calcination temperature and atmosphere on CO-PROX activity of catalysts based on copper and ceria combinations in inverse configurations has been analysed by different techniques. TG-DTA results reveal important differences as a function of the calcination atmosphere (diluted oxygen or inert gas). While an important weight loss is produced in any case above *ca.* 180 °C, mainly related to combustion of microemulsion-derived organic residues, air appears far more effective to decompose such residues, according also to DRIFTS analysis. XRD examination reveals the formation of copper and cerium oxides above *ca.* 200 °C under the two calcination atmospheres. Nevertheless, important differences are related to formation of metallic copper only under inert atmosphere. Catalytic differences for the CO-PROX process are evidenced as a function of the calcination temperature and atmosphere. Thus, catalysts treated under air between 300 and 500 °C display relatively similar CO oxidation activities, despite the important S_{BET} decrease observed with increasing calcination temperature; however, appreciable differences are found in terms of selectivity towards CO_2 formation which is shown to increase with increasing calcination temperature in that range. This can be related to CuO particle size effects on their reducibility under H_2, as independently confirmed by H_2-TPR tests. Very poor CO-PROX activities are however detected for catalysts calcined under air above 500 °C (as a consequence of sintering) or for the catalyst calcined under inert gas at 500 °C (as a consequence of metallic copper or organic residues poisons presence).

Acknowledgements

A.L.C. thanks the CSIC for a JAE PhD grant under which his contribution to this work was done. ICP-CSIC Laboratorio de Análisis Térmico and Unidad de Apoyo are acknowledged for performing TG-DTA and XRD experiments, respectively. Thanks are due to the MICINN (project CTQ2009-14527), Comunidad de Madrid (project DIVERCEL S2009/ENE-1475) and CSIC-HAS bilateral agreement for financial support.

References

[1] J.R. Rostrup-Nielsen, J. Sehested, J.K. Norskov, Adv. Catal. 47 (2002) 65.
[2] Q. Fu, H. Saltsburg, M. Flytzani-Stephanopoulos, Science 301 (2003) 935.
[3] G. Avgouropoulos, T. Ioannides, Ch. Papadopoulou, J. Batista, S. Hocevar, H.K. Matralis, Catal. Today 75 (2002) 157.
[4] S.H. Oh, R.M. Sinkevitch, J. Catal. 142 (1993) 254.
[5] A. Martínez-Arias, A.B. Hungría, M. Fernández-García, J.C. Conesa, G. Munuera, J. Power Sources 151 (2005) 32.
[6] F. Mariño, C. Descorme, D. Duprez, Appl. Catal. B 58 (2005) 175.
[7] A. Martínez-Arias, D. Gamarra, M. Fernández-García, A. Hornés, P. Bera, Zs. Koppány, Z. Schay, Catal. Today 143 (2009) 211.
[8] W. Liu, M. Flytzani-Stephanopoulos, Chem. Eng. J. 64 (1996) 283.
[9] D. Gamarra, C. Belver, M. Fernández-García, A. Martínez-Arias, J. Am. Chem. Soc. 129 (2007) 12064.
[10] D. Gamarra, G. Munuera, A.B. Hungría, M. Fernández-García, J.C. Conesa, P.A. Midgley, X.Q. Wang, J.C. Hanson, J.A. Rodríguez, A. Martínez-Arias, J. Phys. Chem. C 111 (2007) 11026.
[11] A. Martínez-Arias, A.B. Hungría, G. Munuera, D. Gamarra, Appl. Catal. B 65 (2006) 207.
[12] D. Gamarra, A. Hornés, Zs. Koppány, Z. Schay, G. Munuera, J. Soria, A. Martínez-Arias, J. Power Sources 169 (2007) 110.
[13] A. Hornés, A.B. Hungría, P. Bera, A. López Cámara, M. Fernández-García, A. Martínez-Arias, L. Barrio, M. Estrella, G. Zhou, J.J. Fonseca, J.C. Hanson, J.A. Rodriguez, J. Am. Chem. Soc. 132 (2010) 34.
[14] M. Luo, J. Ma, J. Lu, Y. Song, Y. Wang, J. Catal. 246 (2007) 52.
[15] Y. Yu, T. Takei, H. Ohashi, H. He, X. Zhang, M. Haruta, J. Catal. 267 (2009) 121.
[16] X. Xie, Y. Li, Z.-Q. Liu, M. Haruta, W. Shen, Nature 458 (2009) 746.
[17] S. Bernal, J.J. Calvino, J.M. Gatica, C. López Cartes, J.M. Pintado, in: A. Trovarelli (Ed.), Catalysis by Ceria and Related Materials, Imperial College Press, London, 2002, p. 85.
[18] P. Bera, A. Hornés, A. López Cámara, A. Martínez-Arias, Catal. Today 155 (2010) 184.
[19] C.R. Jung, J. Han, S.W. Nam, T.-H. Lim, S.-A. Hong, H.-I. Lee, Catal. Today 93–95 (2004) 183.